HAYATI
Journal of Biosciences

Vol. 32 No. 6, November 2025 1663-1673
DOI:10.4308/hjb.32.6.1663-1673
ISSN: 1978-3019
EISSN: 2086-4094

Research Article

Check for updates

OPEN ACCESS

Osteological Development of Yellow Rasbora Fish *Rasbora lateristriata* (Bleeker, 1854) Treated with Mangosteen *Garcinia mangostana* L. Peel Simplicia

Pradnya Paramita, Luthfia Uswatun Khasanah, and Bambang Retnoaji*

Faculty of Biology, Universitas Gadjah Mada, Jalan Teknika Selatan, Sekip Utara, Yogyakarta 55281, Indonesia

ARTICLE INFO

Article history:
Received July 8, 2024
Received in revised form July 17, 2025
Accepted July 28, 2025
Available Online September 3, 2025

KEYWORDS:
Bone structure,
Mangosteen peel extract,
Rasbora lateristriata,
Toxicity test

ABSTRACT

Mangosteen peel simplicia (*Garcinia mangostana* L.) contains potential ingredients used in medicine. A toxicity test of mangosteen peel simplicia is needed before it is used. Wader pari (*Rasbora lateristriata*) is a potential animal model for toxicity testing. Thus, this study aims to determine the effect of mangosteen peel extract at various concentrations on the behavior and bone structure of *R. lateristriata*. In this research, fish behavior was observed at 48 hpf (hours post-fertilization) and 30 dpf (days post-fertilization). Bone structure observed at 96 hpf, 7 dpf, 14 dpf, 21 dpf, 28 dpf, 35 dpf, and 42 dpf using the Alizarin Red – Alcian Blue method. Observation data on behavior and bone structure were analyzed descriptively, while the number of vertebrae was analyzed quantitatively using One-Way ANOVA ($P < 0.05$). The results showed that the ossification of cranium and caudal complex skeleton components in the 1 and 5 µg/mL treatments was significantly behind that of the control and 0.5 µg/mL treatments. Furthermore, 5 µg/mL treatment caused some behavioral and swimming pattern abnormalities in 48 hpf larvae. In conclusion, exposure to 1 and 5 µg/mL mangosteen peel simplicia resulted in skeletal growth inhibition in *R. lateristriata*. Exposure to 5 µg/mL mangosteen peel simplicia caused abnormalities in the behavior and swimming pattern of 48 hpf larvae.

1. Introduction

Mangosteen, a tree native to Southeast Asia, is widely used in medicine to treat gonorrhea, cysts, wounds, diarrhea, and parasitic infections (Obolskiy *et al*. 2009; Murthy *et al*. 2018). It contains substances with potential anti-inflammatory, antibacterial, anticancer, antifungal, and antioxidant properties, such as xanthones (Obolskiy *et al*. 2009; Widowati *et al*. 2016; Ansori *et al*. 2020; Taokaew *et al*. 2021). However, following WHO guidelines and the Indonesian Ministry of Health Regulation No. 760/menkes/per/IX/1992, further research is required to fully comprehend the impacts of these substances (Mustapa *et al*. 2018).

Several toxicity studies on mangosteen pericarp have shown mixed results across different animal models. Jujun *et al*. (2008) found no significant effects on body weight, organ histopathology, or biochemical and haematological parameters in adult Sprague-Dawley rats. In contrast, Jose *et al*. (2016) reported growth retardation, movement limitations, and malformation in zebrafish. Studies by Lestari *et al*. (2021) and Idrus and Kiswanjaya (2016) demonstrated that α-mangosteen could enhance bone

* Corresponding Author
E-mail Address: bambang.retnoaji@ugm.ac.id

volume and reduce bone destruction in rats and mice. Azhar *et al*. (2017) found that combining mangosteen extract with DFDBBX positively affected bone cells in guinea pigs. Gutierrez-Orozco *et al*. (2013) noted that α-mangosteen's anti-inflammatory properties might inhibit bone formation. The varying results across species suggest the need for further research using different animal models to understand the effect of mangosteen fully.

Rasbora lateristriata, commonly known as yellow rasbora, is a freshwater fish endemic to Indonesia that belongs to the Cyprinidae family. This species is easy to breed, produces numerous eggs, and is highly sensitive to environmental changes, making it an ideal animal model for toxicity tests and drug development (Rahajeng and Retnoaji 2021). Due to these advantages, the yellow rasbora has been widely used in research. Therefore, this study aims to investigate the effects of mangosteen peel simplicial on the osteological development of yellow rasbora and to assess its potential as a natural agent for promoting bone growth and development in aquatic species.

2. Materials and Methods

2.1. Materials and Tools

Materials needed are as follows, mangosteen pericarp powder (Bina Agro), egg water 0.815 g $MgSO_4$, 5.0 g NaCl, 0.15 g KCl, 0.26 g $CaCl_2.{}_2H_2$, 500 mL distilled water, tetramin fish food, 25-30 yellow rasbora broodstock, alizarin red−alcian blue double staining, 96% alcohol, bleaching solution (1:1 of 3% H_2O_2 and 2% KOH), clearing solution (KOH 0.05%), mol solution (20 mL 20% Glycerol, 1% 1 mL KOH and 79 mL distilled water), and 85% glycerol.

Tools needed are as follows: fish maintenance set, light microscope, Leica microscope (Leica DM750), petri dish, watch glass, 6-well plate, microtube, pipette, tweezers, analytical scales, millimeter blocks, beaker, measuring cup, Erlenmeyer, and funnel.

2.2. Fish Maintenance and Spawning

Yellow rasbora broodstock were maintained on a 14-10 light–dark cycle, with a temperature of 27–28.5°C, and dissolved oxygen at 6-8 ppm. Fish were fed tetramine food twice a day. Water quality management was carried out by siphoning and water replacement (Retnoaji *et al*. 2023).

Spawning was carried out using 25-30 yellow rasbora broodstock that were taken from the pond. Females and males broodstock were selected by massaging the abdomen. The ratio used in this spawning is 2:1 male-to-female. The spawning process was performed by placing the selected broodstock in the water-circulated breeding chamber during the afternoon hours, between 4:00 and 5:00 pm—the spawned eggs collected in the next morning (Retnoaji *et al*. 2023). Regular eggs were selected using a light microscope to obtain normal eggs for the treatment.

2.3. Mangosteen Pericarp Extract Preparation and Embryo Treatment

Approximately 100 mg of mangosteen pericarp powder was boiled in 500 mL of distilled water at 90°C for 30 minutes. Then, the stock solution was diluted into four concentration, 0.5, 1, 5, and 25 µg/mL. Each of the four concentrations was exposed to 10 embryos aged 2.5 hours post-fertilization (hpf) for 48 hours using a 6-well plate. An additional 10 embryos were also included as a control group. Each treatment group was administered three times (Suwignyo 2014).

2.4. Bone Structure Observation

Three samples from each treatment aged 96 hpf, 7, 14, 21, 28, 35, and 42 dpf (days post fertilization) were collected and anesthetized using the cold shock method. Then, samples were fixed using 96% alcohol for two days at room temperature. After two days, the fixative solution was discarded and replaced by alizarin red-alcian blue double staining. The samples were stored in dye solution for 3 days at room temperature. Afterwards, the dye solution was removed and washed three times with distilled water. The samples were then added to the bleaching solution and left open for 10 to 120 minutes (depending on the sample size). The bleaching solution was then discarded and replaced by a clearing solution for 5 to 45 minutes. After that, the clearing solution was replaced with a mole solution and left for 12 to 24 hours. Subsequently, the samples were stored in 85% glycerol solution. A few days later, the samples were ready to be observed using a Leica microscope.

2.5. Data Analysis

Data analysis was carried out qualitatively and quantitatively. Qualitative data was obtained from bone structure and behavior observations, which were

descriptively analysed and compared to the control treatment. Quantitative data obtained from the number of vertebrae was analysed using one-way ANOVA (IBM SPSS) to see the significance ($P < 0.05$) of the effect of treatment.

3. Results

Based on the observations, it is known that 25 µg/mL treatment on yellow rasbora resulted in mass death within 48 hours. Due to this result, they could not be maintained further and were stained with alizarin red-alcian blue double staining, while the four other treatments were left intact. Figure 1 shows that the control, 0.5, 1, and 5 µg/mL treatments did not exhibit any differences in bone growth. At this age, it appears that the ethmoid plate is still in the form of cartilage. Several other cartilages that appear in the four treatments include notochord, Meckel's cartilage, interhyal, palatoquadrate, pterygoid process, metapterygoid process, quadrate process, basihyal, ceratohyal, hyosymplectic, basibranchial, hypobranchial, ceratobranchial, posterior basicapsular commissure, parachordal, trabeculae, scapulacoracoid, and radial. Moreover, several bones have undergone development, including the parashenoid, dentary, maxilla, entopterygoid, branchiostegal ray, ceratobranchial teeth, opercle, and cleithrum. 3.2 FRET Immunosensor.

On 7 dpf observations, the control treatment appeared to show the development of a cartilaginous epiphyseal bar (Figure 2B), whereas the other treatments did not show any development (Figure 2E, H, K). Cartilaginous epiphyseal bar on 0.5, 1, and 5 µg/mL treatments developed later on 14 dpf observation (Figure 3). At this age, the anterior end of the notochord also begins to ossify and becomes the perichordal bone, forming the vertebral centrum. This appeared to occur only in the control and 0.5 µg/mL treatments, while the other two treatments had not experienced further ossification. The two treatments also showed exoccipital, ectopterygoid, Weberian apparatus, and vertebral column component development for the

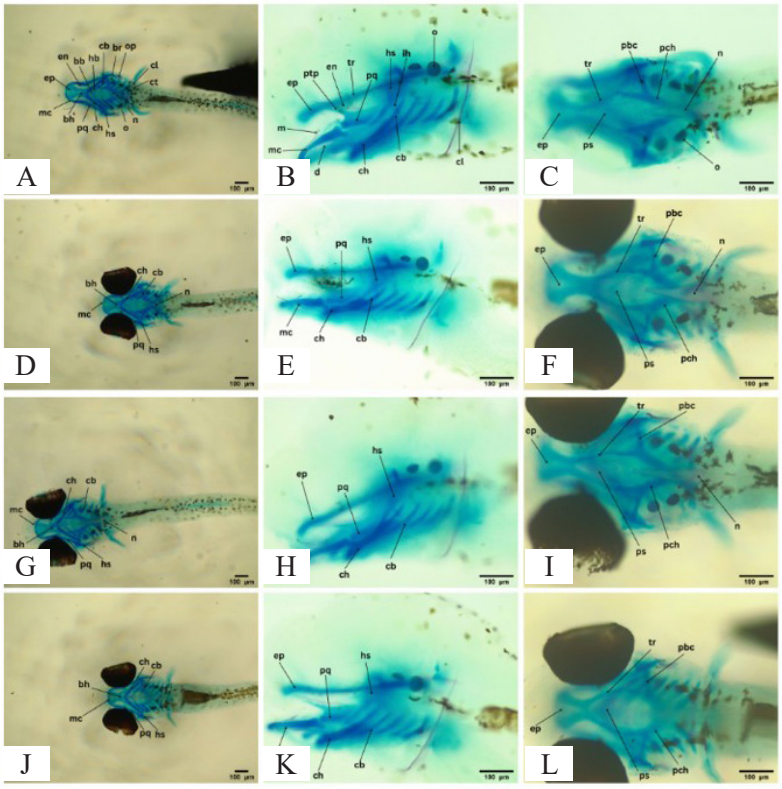

Figure 1. Bone morphology and mineral deposition of 96 hpf yellow rasbora treated with mangosteen pericarp extract. A-C showing the development of the control treatment. D-F showing development of 0.5 µg/mL treatment. G-I showing development of the 1 µg/mL treatment. J-L showing the development of 5 µg/mL treatment. bb = basibranchial, bh = basihyal, br = branchiostegal ray, cb = ceratobranchial, ch = ceratohyal, cl = cleithrum, ct = ceratobranchial teeth, d = dentary, en = entopterygoid, ep = ethmoid plate, hb = hypobranchial, hs = hyosymplectic, ih = interhyal, m = maxilla, mc = meckel's cartilage, n = notochord, o = otolith, op = opercle, pbc = posterior basicapsular commissure, pch = parachordal, pq = palatoquadrate, ps = parashpenoid, ptp= pterygoid process, tr = trabeculae

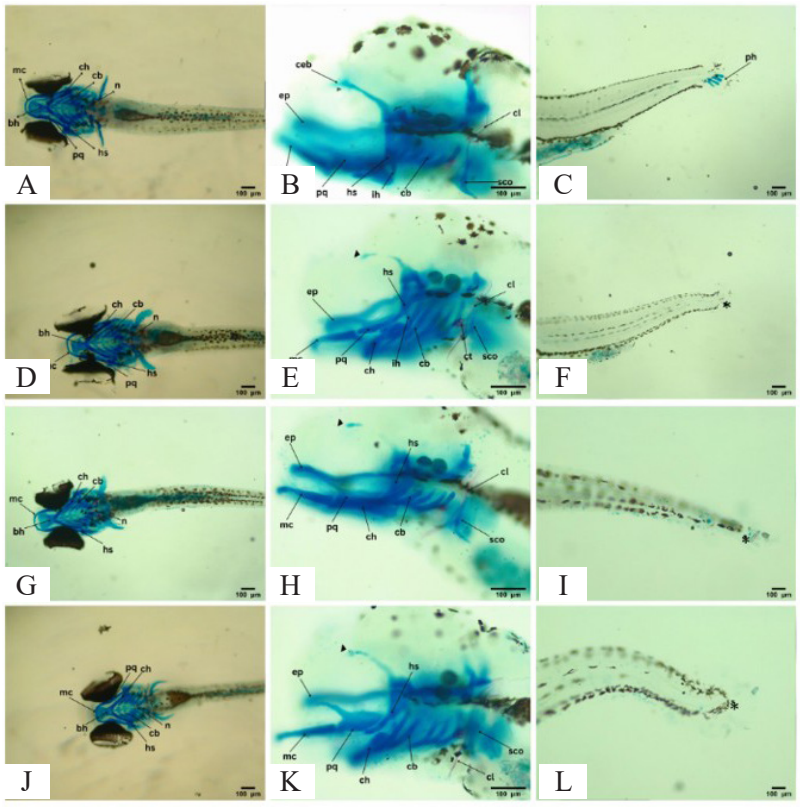

Figure 2. Bone morphology and mineral deposition of 7 dpf yellow rasbora treated with mangosteen pericarp extract. A-C showing the development of the control treatment. D-F showing the development of 0.5 µg/mL treatment. G-I showing development of the 1 µg/mL treatment. J-L showing the development of 5 µg/mL treatment. Asterisk sign (*) showing parahypertro absent. bh = basihyal, cb = ceratobranchial, ceb = cartilaginous epiphyseal bar, ch = ceratohyal, cl = cleithrum, ct = ceratobranchial teeth, ep = ethmoid plate, hs = hyosymplectic, ih = interhyal, mc = meckel's cartilage, n = notochord, ph = parhypural, pq = palatoquadrate, ps = parashpenoid

first time, while the pterygoid process was perfectly developed. Apart from the differences in bone growth among the four treatments, the premaxilla was found to be developed in all four treatments.

Figure 4 shows the development of the basipterygium in the control treatment at 21 dpf. Kinethmoid, frontal, and nasal also began to develop and stained blue at control and 0.5 µg/mL treatments. The orbitosphenoid, pterosphenoid, pectoral ray, rib, neural arch, hemal arch, dorsal ray, anal ray, and urostyle appeared red in the same two treatments. Hyosimplectic and hyomandibular in both treatments became stained red, indicating further ossification of the bone matrix. The ectopterygoid, Weberian apparatus, pterygiophore, epural, preural, centrum, vertebral centrum, and caudal ray in 1 and 5 µg/mL treatments finally showed development.

Observation on control and 0.5 µg/mL treatments at 28 dpf showed that the supraorbital, postcleithrum, and pectoral rays began to develop (Figure 5). Basihyal and symplectic began to show further ossification in the control treatment. It could be seen from the edges of the basihyal, which started to turn red, while the middle part remained blue. Ceratohyal, epiral, and hypural in the control and 0.5 µg/mL treatments also exhibited the same ossification as the basihyal. The pectoral ray, rib, neural arch, hemal arch, dorsal ray, anal ray, and urostyle, which had not previously developed in the 1 and 5 µg/mL treatments, showed development. Furthermore, basipterygium began to appear in the 0.5 and 1 µg/mL treatments.

Frontal development in the control and 0.5 µg/mL treatments continued at 35 dpf (Figure 6). The supraorbital, which had previously still stained blue, became stained red in the same two treatments. The palatoquadrate and parhypural underwent further ossification, showing a partially red color in both treatments as well. Basipterygium began to be observed at concentrations of 5 µg/mL. Nasal, orbitoshpenoid, pterosphenoid, and supraorbital began to develop at 42 dpf (Figure 7). Apart from the development of some of the bones above, no new bone growth was seen in the control and 0.5 µg/mL treatments.

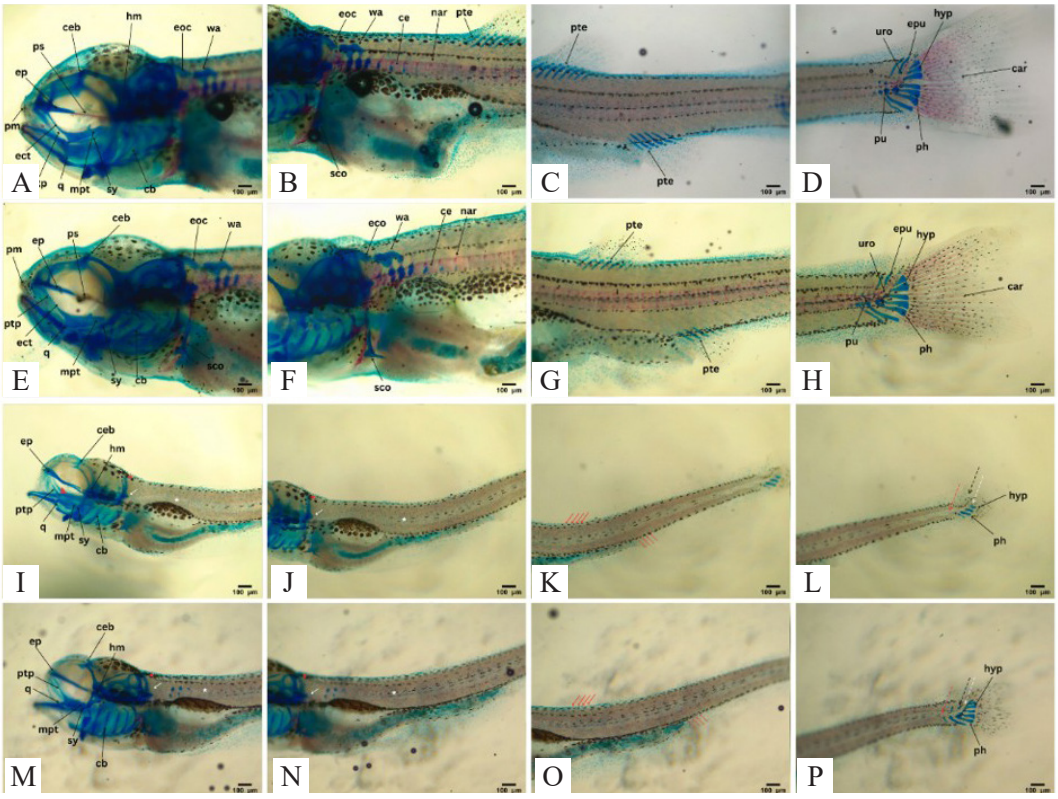

Figure 3. Bone morphology and mineral deposition of 14 dpf yellow rasbora treated with mangosteen pericarp extract. A-D showing the development of the control treatment. E-H showing the development of 0.5 µg/mL treatment. I-L showing development of 1 µg/mL treatment. M-P showing the development of 5 µg/mL treatment. (Red asterisk) eoc. (Red arrowhead) ect. (White arrow) wa. (White asterisk) ce. (Red dashed arrow) pte. (Black dashed arrow) epu. (White dashed arrow) uro. car = caudal ray, cb = ceratobranchial, ce = centrum, ceb = cartilaginous epiphyseal bar, ect = ectopterygoid, eoc = exoccipital, ep = ethmoid plate, epu = epural, hm = hyomandibular, hyp = hypural, mpt = metapterygoid, nar = neural arch, ph = parhypural, pm = premaxilla, ps = parasphenoid, pte = pterygiophore, ptp = pterygoid process, pu = preural centrum, q = quadrate, sco = scapulacoracoid, sy = symplectic, uro = urostyle, wa = weberian apparatus

However, ossification of the matrix of each part of the bone continued.

Based on the observations, it is known that at 96 hpf and 7 dpf, the vertebral column had not undergone ossification (Figure 8). The structural units of the vertebral column began to appear at 14 dpf in the control and 0.5 µg/mL treatments. In contrast, the 1 and 5 µg/mL treatments did not show any mineral deposition, making it hard to count the number of vertebrae. The control and 0.5 µg/mL treatments had approximately 33-34 vertebrae. ANOVA analysis revealed significant differences in the 1 and 5 µg/mL treatments compared to the control and 0.5 µg/mL treatments at 14 dpf due to a lack of mineral deposition. At 21 and 42 days post-fertilization (dpf), vertebrae counts were approximately 34-35, with no significant differences among treatments. At 28 and 35 days post-fertilization (dpf), counts ranged from 32 to 35 vertebrae, and statistical analysis showed no significant differences between treatments.

Observations of vertebral column ossification revealed that structural ossification of the vertebral column unit first appeared at 14 days post-fertilization (dpf) in both the control and 0.5 µg/mL treatment groups (Table 1). The control and 0.5 µg/mL treatment showed mild ossification in the centrum, neural arches, and hemal arches. On the other hand, treatments at 1 and 5 µg/mL did not show any deposition of mineral structures in the vertebral column unit. At the 21-day post-fertilization (dpf) age, the control and 5 µg/mL treatments showed high ossification of the centrum, neural arches, and hemal arches. In comparison, treatments at 1 and 5 µg/mL only showed centrum development for the first time and were categorized as mild ossification. In these two treatments, the development of the neural and hemal arches was still not visible.

Observations at 28 dpf revealed that both the control and 5 µg/mL treatments exhibited extensive ossification on the centrum, neural, and hemal arches, with the latter being

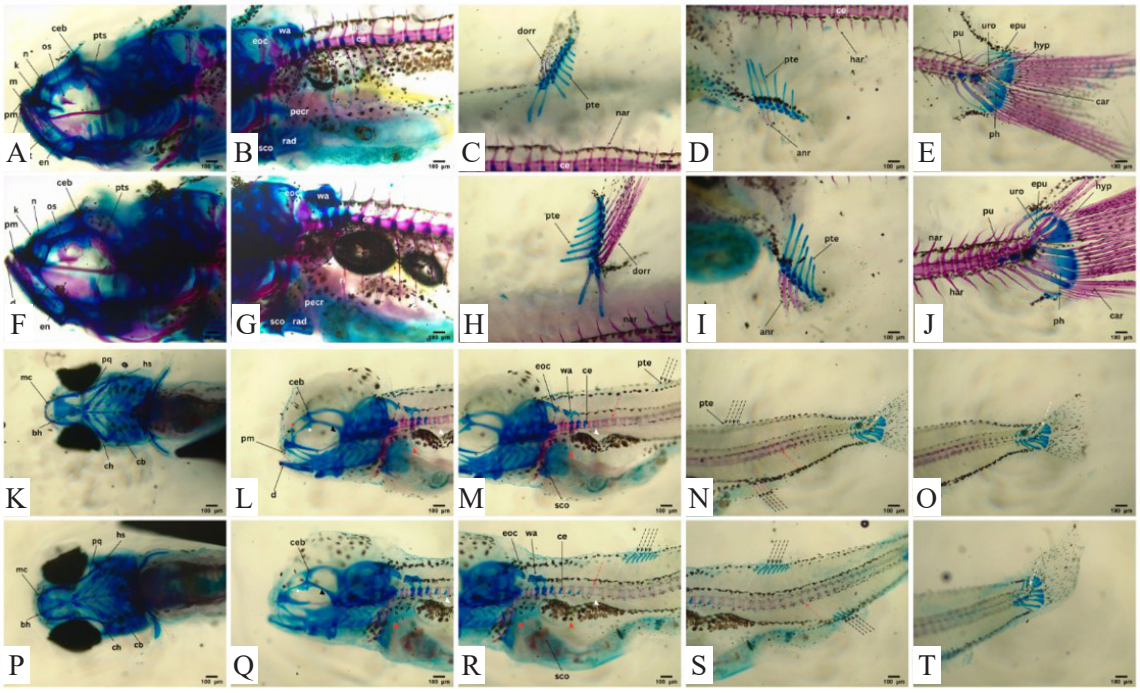

Figure 4. Bone morphology and mineral deposition of 21 dpf yellow rasbora treated with mangosteen pericarp extract. A-E showing the development of the control treatment. F-J showing the development of 0.5 µg/mL treatment. K-O showing development of the 1 µg/mL treatment. P-T showing the development of 5 µg/mL treatment. (Black asterisk) k. (Red asterisk) n. (White asterisk) os. (Black arrowhead) pts. (Red arrowhead) pecr. (White arrowhead) ri. (Black dashed arrow) nar dan har. (White dashed arrow) dorr and anr. (White dashed arrow) uro. anr = anal ray, car = caudal ray, ce = centrum, ceb = cartilaginous epiphyseal bar, d = dentary, dorr = dorsal ray, ect = ectopterygoid, en = entopterygoid, eoc = exoccipital, ep = ethmoid plate, epu = epural, har = hemal arch, hm = hyomandibular, hyp = hypural, k = kinethmoid, m = maxilla, mpt = metapterygoid, n = nasal, nar = neural arch, os = orbitosphenoid, pecr = pectoral ray, ph = parhypural, pm = premaxilla, ps = parasphenoid, pte = pterygiophore, pts = pterosphenoid, pu = preural centrum, q = quadrate, ri = rib, rad = radial, sco = scapulacoracoid, sy = symplectic, uro = urostyle, wa = weberian apparatus

more pronounced (Figure 9). The structural ossification of the units in these two treatments can be described as complete ossification. The 1 and 5 µg/mL treatments showed moderate ossification in the centrum, while the neural and hemal arches showed mild ossification. Control and 0.5 µg/mL treatments showed more complete development of structural ossification of the unit at 35 dpf. Otherwise, treatments at 1 and 5 µg/mL still showed moderate ossification in the centrum and mild ossification in the neural and hemal arches. Finally, at the age of 42 days post-fertilization (dpf), the control and 0.5 µg/mL treatments experienced further development of complete structural ossification of the unit. Treatment 1 µg/mL showed a moderate increase in ossification in the centrum, neural, and hemal arches. On the other hand, 5 µg/mL treatments appeared to show moderate ossification in the centrum, as well as mild ossification in the neural and hemal arches.

4. Discussion

During observation, mass mortality within 48 hours in the 25 µg/mL treatment indicates this concentration was lethal for yellow rasbora, suggesting the lethal threshold may fall between 5 and 25 µg/mL. This is consistent with Nguyen (1999), who reported toxic effects of mangosteen pericarp extract above a certain threshold, potentially causing prooxidant damage. Due to the high mortality at 25 µg/mL, bone structure analysis using alizarin red-alcian blue staining was not possible.

Bone structure analysis focused on chondrocranium, osteocranium, and caudal complex ossification. The chondrocranium, which forms the neurocranium, originates from cartilage that eventually ossifies, while the osteocranium represents the cranial bones. The caudal complex comprises postcranial structures, including the vertebral centrum, fins, and tail (Piekarski *et al*. 2014; Maynard and Downes 2019; Biagio *et al*. 2022).

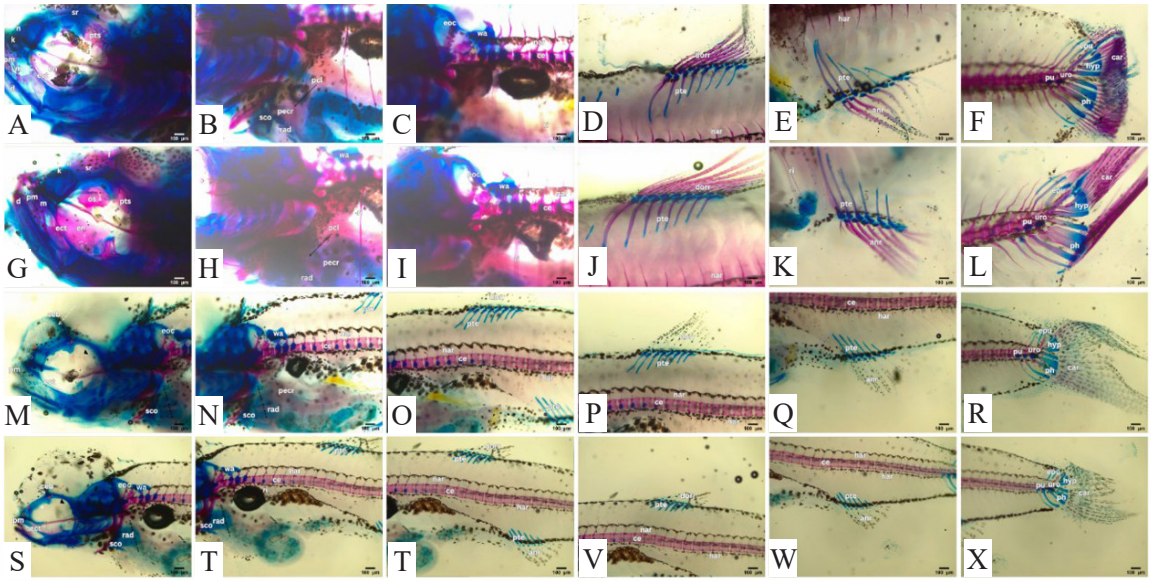

Figure 5. Bone morphology and mineral deposition of 28 dpf yellow rasbora treated with mangosteen pericarp extract. A-F showing the development of the control treatment. G-L showing the development of 0.5 µg/mL treatment. M-R showing development of 1 µg/mL treatment. S-X showing the development of 5 µg/mL treatment. (Black asterisk) k. (Red asterisk) n. (White asterisk) os. (Black arrowhead) pts. (Red arrowhead) pecr. (White arrowhead) ri. (Red dashed arrow) sr. (Black dashed line) pcl. (White dashed arrow) f. anr = anal ray, car = caudal ray, ce = centrum, d = dentary, dorr = dorsal ray, ect = ectopterygoid, en = entopterygoid, eoc = exoccipital, epu = epural, f = frontal, har = hemal arch, hyp = hypural, k = kinethmoid, m = maxilla, n = nasal, nar = neural arch, os = orbitosphenoid, pcl = postcleithrum, pecr = pectoral ray, ph = parhypural, pm = premaxilla, pte = pterygiophore, pts = pterosphenoid, pu = preural centrum, q = quadrate, rad = radial, ri = rib, sco = scapulacoracoid, sr = supraorbital, sy = symplectic, uro = urostyle, wa = weberian apparatus

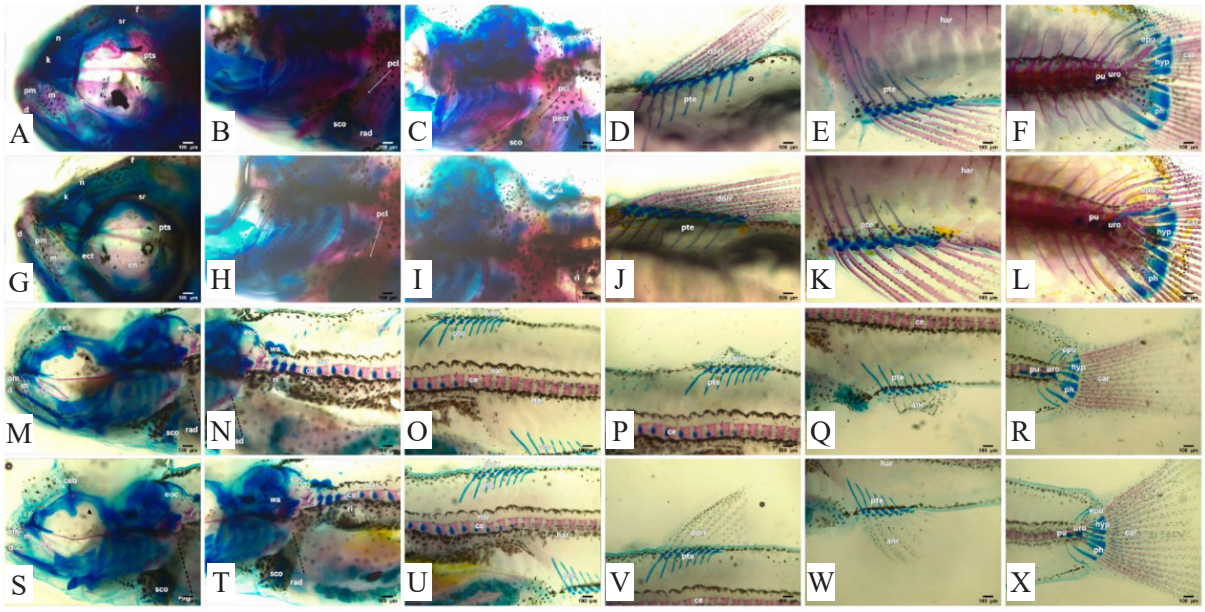

Figure 6. Bone morphology and mineral deposition of 35 dpf yellow rasbora treated with mangosteen pericarp extract. A-F showing the development of the control treatment. G-L showing the development of 0.5 µg/mL treatment. M-R showing development of 1 µg/mL treatment. S-X showing the development of 5 µg/mL treatment. (Black asterisk) k. (Red asterisk) n. (White asterisk) os. (Black arrowhead) pts. (Red arrowhead) pecr. (Red dashed arrow) sr. (Black dashed line) pcl. (White dashed arrow) f. anr = anal ray, car = caudal ray, ce = centrum, ceb = cartilaginous epiphyseal bar, d = dentary, dorr = dorsal ray, ect = ectopterygoid, en = entopterygoid, eoc = exoccipital, epu = epural, f = frontal, har = hemal arch, hyp = hypural, k = kinethmoid, m = maxilla, n = nasal, nar = neural arch, os = orbitosphenoid, pcl = postcleithrum, pecr = pectoral ray, ph = parhypural, pm = premaxilla, pte = pterygiophore, pts = pterosphenoid, pu = preural centrum, q = quadrate, rad = radial, ri = rib, sco = scapulacoracoid, sr = supraorbital, sy = symplectic, uro = urostyle, wa = weberian apparatus

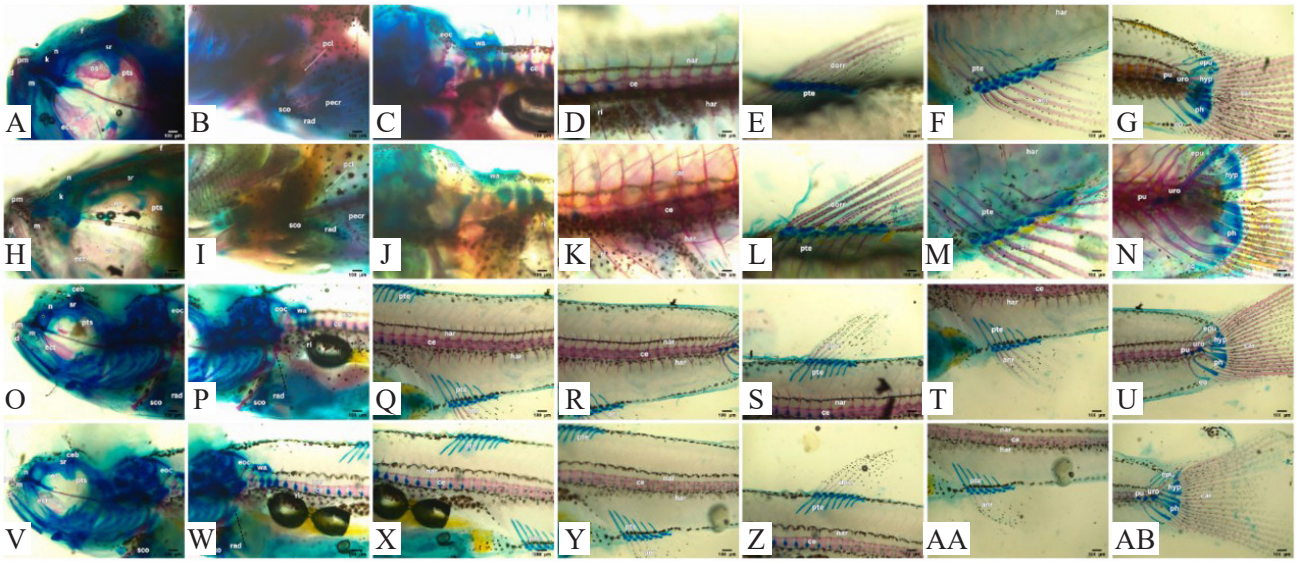

Figure 7. Bone morphology and mineral deposition of 42 dpf yellow rasbora treated with mangosteen pericarp extract. A-G showing the development of the control treatment. H-N showing the development of 0.5 µg/mL treatment. O-U showing the development of a 1 µg/mL treatment. V-AB showing development of 5 µg/mL treatment. (Black asterisk) k. (Black dashed line) pcl. (White dashed arrow) f. anr = anal ray, car = caudal ray, ce = centrum, d = dentary, dorr = dorsal ray, ect = ectopterygoid, en = entopterygoid, eo = extra caudal ossicle, eoc = exoccipital, epu = epural, f = frontal, har = hemal arch, hyp = hypural, k = kinethmoid, m = maxilla, n = nasal, nar = neural arch, os = orbitosphenoid, pcl = postcleithrum, pecr = pectoral ray, ph = parhypural, pm = premaxilla, pte = pterygiophore, pts = pterosphenoid, pu = preural centrum, q = quadrate, rad = radial, ri = rib, sco = scapulacoracoid, sr = supraorbital, sy = symplectic, uro = urostyle, wa = weberian apparatus

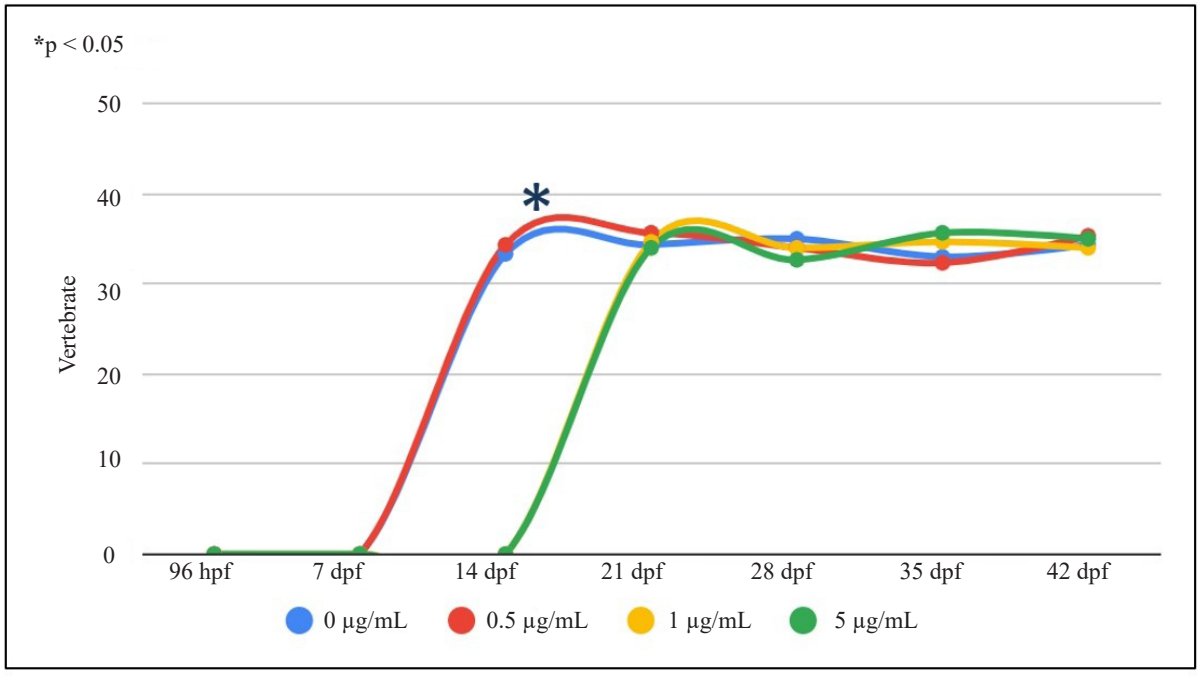

Figure 8. Trend in the number of vertebrae in the four treatments at 96 hpf to 42 dpf. *p < 0.05, indicating significant differences between the control and 0.5 µg/mL treatments compared to the 1 and 5 µg/mL treatments at 14 dpf

Observations of bone development (Figures 1-7) revealed distinct effects of varying concentrations. At 96 hpf, there were no significant differences in skeletal growth across control and lower treatments (0.5, 1, and 5 µg/mL). Key cartilages such as the ethmoid plate and Meckel's cartilage remained prominent. This suggests early skeletal development is resilient to low-dose treatments, aligning with previous studies (Harris and Dorsky 2007).

By 7 dpf, control larvae exhibited cartilaginous epiphyseal bar development, while 0.5, 1, and 5 µg/mL treatments displayed delayed formation, observed by 14 dpf (Figure 3). This delay suggests concentration-dependent inhibition in cartilage development, similar to the effects observed in other fish exposed to various substances (Brunson *et al*. 2015). Initial ossification at lower concentrations indicates potential promotion of early bone formation (Thompson *et al*. 2012). Variation in bone development across treatments may stem from growth inhibition, as bone maturity relates to fish size (Dietrich *et al.* 2021). Growth delay due to mangosteen extracts, previously noted in zebrafish (Jose *et al*. 2016), may be analogous to the inhibition observed in yellow rasbora.

By 21 days post-fertilization (dpf), significant developments, such as basipterygium and skull bones, were evident in both control and 0.5 µg/mL treatments. Continued ossification in these groups, particularly in the basihyal and other bones, contrasts with inhibited maturation in the 1 and 5 µg/mL treatments, supporting the finding that high concentrations can disrupt skeletal maturation (Kwak and Langerhans 2018).

Later stages (28 and 35 dpf) confirmed advanced ossification in both control and 0.5 µg/mL treatments, with higher concentrations showing a lag. By 42 days post-fertilization (dpf), some recovery was noted in the 5 µg/mL group, with the appearance of nasal, orbitosphenoid, and pterosphenoid bones; however, development remained behind that of lower treatments. This delayed recovery may indicate a compensatory mechanism, as observed in similar developmental studies (Hsiesh *et al*. 2019).

The delayed progression in cranial and skeletal development indicates that while overall bone growth may eventually normalize, specific skeletal structures respond variably to different treatment concentrations. Vertebral ossification assessments revealed distinct differences in the timing and degree of development across treatments. At 14 dpf, ossification began in the centrum, neural arches, and hemal arches for both control and 0.5 µg/mL treatments, aligning with the expected skeletal timelines (Harris and Dorsky 2007). However, no mineral deposition occurred in the 1 and 5 µg/mL treatments, suggesting developmental delays consistent with inhibited growth at higher concentrations (Andersen *et al*. 2015; Dietrich *et al*. 2021).

By 21 days post-fertilization (dpf), ossification advanced in the control and 5 µg/mL treatments, while the 1 µg/mL treatment showed only initial ossification in the centrum, reflecting delayed development under higher concentrations (Jose *et al*. 2016; Langerhans *et al*. 2018). At 28 days post-fertilization (dpf), the control and 0.5 µg/mL treatments exhibited extensive ossification in the centrum, neural arches, and hemal arches, reaching what can be considered complete ossification. This suggests that while the 5 µg/mL treatment may initially delay development, it ultimately supports a high level of ossification comparable to that of the control. The 1 µg/mL treatment exhibited moderate ossification in the centrum, while the neural and hemal arches remained only mildly ossified, indicating ongoing developmental challenges at this concentration (Kwak & Langerhans 2018). By 35 days post-fertilization (dpf), both the control and 0.5 µg/mL treatments exhibited complete ossification, but delays persisted in the 1 and 5 µg/mL treatments. At 42 dpf, only the control and 0.5 µg/mL treatments approached complete ossification, whereas the higher concentration showed moderate ossification, underscoring the lasting impact of elevated treatments on skeletal development (Wang *et al*. 2019).

The delays in vertebral ossification at higher concentrations highlight the sensitivity of skeletal development to treatment levels. The lack of mineral deposition in the 1 and 5 µg/mL groups at 14 dpf impacts both ossification timing and vertebral number, reflecting significant developmental disruptions. Assessment of vertebral number showed a significant difference at 14 dpf between the control (0.5 µg/mL) and the 1-5 µg/mL treatments, where mineral deposition was absent, preventing enumeration. In the end, it is known that the vertebral number in yellow rasbora ranges from 32 to 35. However, these findings suggest broader implications for skeletal formation in yellow rasbora and highlight the need for further research on the long-term effects on bone structure and growth.

The delayed mineral deposition in vertebrae suggests a disruption in the skeletal maturation process, which may also influence other physiological systems that rely on proper skeletal support and structural integrity. Since bone development is intertwined with broader

physiological stability, such structural delays could potentially cascade into observable effects on motor functions and behaviors, particularly in larval stages when both skeletal and neural systems are still maturing.

Behavioral observations of 48 hpf larvae under 5 µg/mL treatment displayed abnormal swimming patterns, including circling, sideways swimming, seizures, and C-start responses. Abnormal, repetitive C-start behavior indicates heightened sensory sensitivity, possibly due to motor or sensory system dysfunction (Kalueff *et al*. 2013; Walmsley *et al*. 2020). While swimming sideways, lateral movement exposing one eye suggests swim bladder dysfunction (Retnoaji *et al*. 2023). Seizure-like behavior, marked by convulsive movements with minimal progression, suggests neural disruption and potentially neurotoxic effects of the extract (Kalueff *et al*. 2013; Zhang *et al*. 2021). These behavioral anomalies offer further insight into how elevated treatment concentrations not only hinder skeletal development but also induce neurophysiological disruptions in aquatic organisms.

In summary, the results of this study reveal significant impacts of mangosteen pericarp on both the skeletal development and behavior of yellow rasbora. Lower concentrations permitted normal bone growth and behavioral patterns, whereas higher concentrations led to inhibited ossification and noticeable behavioral abnormalities. However, uncertainties remain regarding the precise mechanisms behind these effects and the long-term implications for fish health and development. These findings underscore the need for further research to clarify these mechanisms, assess the full extent of the impact, and explore potential recovery or adaptation strategies. Understanding these aspects is crucial for evaluating the ecological and health implications of natural substances in aquatic environments and ensuring safe and sustainable practices.

Acknowledgements

Thank you to the Rekognisi Tugas Akhir (RTA) for providing funding for this project. The author also wishes to extend profound and sincere appreciation to the Faculty of Biology, Universitas Gadjah Mada, and Gamawader members for the facilities and all assistance during the experiment and writing the manuscript.

References

Andersen, L., Knudsen, E., Bergh, O., 2015. The impact of environmental pollutants on bone development in fish. *Marine Pollution Bulletin*. 97, 93-101.

Ansori, A.N.M., Fadholly, A., Hayaza, S., Susilo, R.J.K., inayatillah, B., Winarni, D., Husen. S.A., 2020. A review on medicinal properties of mangosteen (*Garcinia mangostana* L.) *Research J. Pharm. and Tech*. 13, 974-982. https://doi.org/10.5958/0974-360X.2020.00182.1

Azhar, I.S., Kresnoadi, U., Rahayu, R.P., 2017. Potency of *Garcinia mangostana* L. peel extract combined with demineralized freeze-dried bovine bone xenograft on IL-1β expression, osteoblasts, and osteoclasts in alveolar bone. *Dental Journa*l. 50, 166-170. https://doi.org/10.20473/j.djmkg.v50.i3.p166-170

Biagio, C.D., Dellacqua, Z., Martini, A., Huysseune, A., Scardi, M., Witten, P.E., Boglione, C., 2022. A baseline for skeletal investigations in Medaka (*Oryzias latipes*): the effects of rearing density on the postcranial phenotype. *Frontiers in Endocrinology*. 13, 1-20. https://doi.org/10.3389/fendo.2022.893699

Brunson, K., Smith, M., Johnson, R., 2015. Effects of environmental contaminants on early fish development. *Aquatic Toxicology*. 164, 69-78.

Dietrich, K., Fiedler, I.A., Kurzyukova, A., Lopez-Delgado, A.C., McGowan, L.M., Geurtzen, K., Hammond, C.L., Busse, B., Knopf, F., 2021. Skeletal biology and desease modeling in zebrafish. *Journal of Bone and Mineral Research*. 36, 436-458. https://doi.org/10.1002/jbmr.4256

Gutierrez-Orozco, F., Chitchumroonchokchai, C., Lesinski, G.B., Suksamrarn, S, Failla, M.L. 2013. α-Mangostin: anti-inflamatory activity and metabolism by human cells. *Journal of Agricultural and Food Chemistry*. 61, 3891-3900. https://doi.org/10.1021/jf4004434

Harris, M.P., Dorsky, R. I., 2007. Early stages of skeletal development in zebrafish. *Journal of Developmental Biology*. 18, 235-245.

Hsieh, S., Wang, C., Yang, Y., 2019. Recovery and compensatory growth in fish exposed to high concentrations of environmental stressors. *Marine Biology*. 166, 50.

Idrus, E., Kiswanjaya, B., 2016. Mangosteen extract inhibits LPS-induced bone resorption by controlling osteoclast. *Journal of International Dental and Medical Research*. 9, 362-367.

Jose, B.V., Dulay, R.M.R., David, E.S., 2016. Toxic and teratogenic assessment of mangosteen (*Garcinia mangostana* L.) leaves and stem-bark lyophilized water extracts in zebrafish (*Danio rerio*) embryos. *Advance in Environmental Biology.* 10, 96-101.

Jujun, P., Pootakham, K., Pongpaibul, Y., Duangrat, C., Tharavichitkul, P., 2008. Acute and repeated dose 28-day oral toxicity of *Garcinia mangostana* Linn. Rind extract. *Cmu. J. Nat. Sci*. 7, 199-208.

Kalueff, A.V., Stewart, A.M., Raju, I., 2013. The role of zebrafish in neuropharmacology research. *Neuropharmacology*, 75, 36-42.

Kalueff, A.V., Gebhardt, M., Stewart, A.M., Cachat, J.M., Brimmer, M., Chawla, J.S., Craddock, C., Kyzar, E.J., Roth, A., Landsman, S., Gaikwad, S., Robinson, K., Baatrup, E., Tierney, K., Shamchuk, A., Norton, W., Miller, N., Nicolson, T., Braubach, O., Gilman, C.P., Pittman, J., Rosemberg, D.B., Gerlai, R., Echevarria, D., Lamb, E., Neuhauss, S.C.F., Weng, W., Bally-Cuif, L., Schneider, H., 2013. Towards a comprehensive catalog of zabrafish behavior 1.0 and beyond. *Zebrafish*. 10, 70-86.

Kwak, J., Langerhans, R.B., 2018. Dose-dependent effects of pollutants on fish bone growth. *Environmental Science & Technology*. 52, 4567-4575.

Langerhans, R.B., Smith, C., Wright, J., 2018. Delayed skeletal development in fish exposed to elevated contaminants. *Aquatic Toxicology*. 194, 34-42.

Lestari, C., Darwin, E., Putra, D.P., Suharti, N., 2021. The α-mangostin effect on the quantity of TGF-β1 titer relate to the mandibular bone volume of Rattus norvegicus in the periodotitis model. *Journal of Pharmacy & Pharmacognosy Research*. 9, 609-618. https://doi.org/10.56499/jppres21.1015_9.5.609

Maynard, R.L., Downes, N., 2019. *Anatomy and Histology of the Laboratory Rat in Toxicology and Biomedical Research,* First ed. Elsevier Inc. London.

Murthy, H.N., Dandin, V.S., Dalawai, D., Park, S-Y., Paek, K-Y. 2018. Breeding of *Garcinia* spp. In: Al-Khayri, J.M., Jain, S.M., Johnson, D.V., (Eds.), *Advance in Plant Breeding Strategies: Fruits*. New York: Springer International Publishing AG. pp. 773-809.

Mustapa, M.A., Tuloli, T.S., Mooduto, A.M., 2018. Uji toksisitas akut yang diukur dengan penentuan Ld50 ekstrak etanol bunga cengkeh (*Syzygium aromaticum* L.) terhadap mencit (*Mus musculus*) menggunakan metode Thompson-Weil. *Jurnal Sains dan Teknologi, Universitas Negeri Manado*. 1, 1-13. https://doi.org/10.36412/frontiers/001035e1/april201801.10

Nguyen, H.H., Widodo, S., 1999. *Medicinal and poisonous plant research of South-East Asia 12*. Pudoc Scientif Publisher, Wageningen.

Obolskiy, D., Pischel, I., Siriwatanametanon, N., Heinrich, M. 2009. *Garcinia mangostana* L.: A phytochemical and pharmacological review. *Phytotheraphy Research*. 23, 1047-1065. https://doi.org/10.1002/ptr.2730

Piekarski, N., Gross, J.B., Hanken, J., 2014. Evolution innovation and conservation in the embryonic derivation of the vertebrate skull. *Nature Communications*. 5, 1-9. https://doi.org/10.1038/ncomms6661

Rahajeng, A., Retnoaji, B., 2021. The effect of dioscorea alata extract on the early development of zebrafish embryo (*Danio rerio*) and *Rasbora lateristriata*. *Advances in Social Science, Education and Humanities Research*, 536, 601-611. https://doi.org/10.2991/assehr.k.210312.096

Retnoaji, B., Paramita, P., Khasanah, L.U., 2023. Mangosteen *Garcinia mangostana* L. simplicia effect on bone structure and behavior of wader fish *Rasbora lateristriata* (Bleeker, 1854) embryo. *Indonesian Journal of Pharmacy*. 34, 182-192. https://doi.org/10.22146/ijp.6348

Suwignyo, A., 2014. Uji toksisitas ekstrak etanol kulit manggis (*Garcinia mangostana*) pada embrio zebrafish (*Danio rerio*) [Sarjana thesis]. Universitas Brawijaya.

Taokaew, S., Chiaoprakobkij, N., Siripong, P., Sanchavanakit, N., Pavasant, P., Phisalaphong, M., 2021. Multifunctional cellulosic nanofiber film with enhanced antimicrobial and anticancer properties by incorporation of ethanolic extract of *Garcinia mangostana* peel. *Master Sci. Eng. C. Mater. Biol. Appl*. 120, 111783. https://doi.org/10.1016/j.msec.2020.111783

Thompson, T.K., Bowers, A., Fagan, M., 2012. Bone development in fish under controlled environmental conditions. *Fish Physiology and Biochemistry*. 38, 1229-1240.

Walmsley, J.J., White, R.W., McCormick, C.L., 2020. The impact of environmental stressors on fish behavior: Insights from zebrafish and other species. *Aquatic Toxicology*. 224, 105493.

Wang, J., Li, H., Zheng, Y., 2019. Effects of environmental stressors on fish bone development. *Journal of Fish Diseases*. 42, 1457-1470.

Widowati, W., Darsono, L., Suherman, J., Fauziah, N., Maesaroh, M., Erawijantari, P.P., 2016. Anti-inflammatory effect of mangosteen (*Garcinia mangostana* L.) peel extract and its compounds in LPS-induced RAW264.7 cells. *Natural Product Science*. 22, 147-153. https://doi.org/10.20307/nps.2016.22.3.147

Zhang, W., Zhang, M., Zhang, Y., 2021. Neurotoxic effects of environmental contaminants on fish behavior: A review. *Environmental Pollution*. 276, 116640.